ACS APPLIED MATERIALS & INTERFACES

Research Article

www.acsami.org

Charge Transfer-Induced Molecular Hole Doping into Thin Film of Metal–Organic Frameworks

Deok Yeon Lee,[†] Eun-Kyung Kim,[†] Nabeen K. Shrestha,*[,†] Danil W. Boukhvalov,*[,†] Joong Kee Lee,[‡] and Sung-Hwan Han*[,†]

[†]Department of Chemistry, Hanyang University, Seoul 133-791, Republic of Korea

[‡]Energy Storage Research Center, Korea Institute of Science and Technology, Seoul 136-791, Republic of Korea

Supporting Information

ABSTRACT: Despite the highly porous nature with significantly large surface area, metal–organic frameworks (MOFs) can be hardly used in electronic and optoelectronic devices due to their extremely poor electrical conductivity. Therefore, the study of MOF thin films that require electron transport or conductivity in combination with the everlasting porosity is highly desirable. In the present work, thin films of $Co_3(NDC)_3DMF_4$ MOFs with improved electronic conductivity are synthesized using layer-by-layer and doctor blade coating techniques followed by iodine doping. The as-prepared and doped films are characterized using FE-SEM, EDX, UV/visible spectroscopy, XPS, current–voltage measurement, photoluminescence spectroscopy, cyclic voltammetry, and incident photon to current efficiency measurements. In addition, the electronic and semiconductor properties of the MOF films are characterized using Hall Effect measurement, which reveals that, in contrast to the insulator behavior of the as-prepared MOFs, the iodine doped MOFs behave as a p-type semiconductor. This is caused by charge transfer-induced hole doping into the frameworks. The observed charge transfer-induced hole doping phenomenon is also confirmed by calculating the densities of states of the as-prepared and iodine doped MOFs based on density functional theory. Photoluminescence spectroscopy demonstrates an efficient interfacial charge transfer between TiO_2 and iodine doped MOFs, which can be applied to harvest solar radiations.

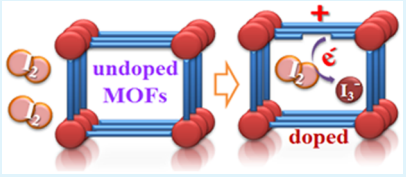

KEYWORDS: *charge transfer complex, molecular hole doping, thin film, MOFs, Hall Effect measurement*

1. INTRODUCTION

Metal–organic frameworks (MOFs) have been studied extensively for many promising applications such as gas storage, gas decontamination/separation, heterogeneous catalysis, photocatalysis, sensors, and electrical energy storage.[1−9] For most of these applications, MOFs are used in the form of bulk powder. One of the interesting and challenging future issues in the field of MOFs is their material investigation for making thin film, and studying their electronic properties.[10−15] However, a huge majority of MOFs are electrically insulators.[16−21] Therefore, despite the highly porous nature with significantly large surface area, MOFs can be hardly used in electronic and optoelectronic devices. Hence, the study of MOF thin films that require electron transport or conductivity in combination with the everlasting porosity is highly desirable. Recently, the concepts of MOFs as potentially active materials in semiconductor science are emerging.[22−26] However, the most challenging issue in MOFs is their poor electrical conductivity, which is needed to be improved to use MOF thin film as a semiconductor material. Some attempts to improve conductivity demonstrate that the conductivity of MOFs can be improved to some extent by molecular doping of the frameworks with electron acceptors, or by using some typical organic linkers.[16−21,27] In addition, modulation of MOF conductivity by changing the metal cations has also been demostrated. For instance, Park et al.[28] have recently demonstrated that the shortest S···S distance between neighboring tetrathiafulvalene cores of tetrathiafulvalene tetrabenzoate-based MOFs can be shortened by using larger cations. This causes an increase in the overlapping between the S $3p_z$ orbitals, and thereby modulates the electrical conductivity of the MOFs from Zn^{2+} to Co^{2+}, Mn^{2+}, and Cd^{2+}. On the other hand, Sun et al.[29] have demonstrated that by changing cations from Mn^{2+} to Fe^{2+} in dihydroxybenzene-1,4-dicarboxylate-based MOFs, electrical conductivity can be enhanced to a million-fold.

In the postsynthetic modification route of electrical conductivity, iodine has been often inserted into MOFs as an electron acceptor molecule, which has demonstrated an improved conductivity of the frameworks as a result of oxidative doping of the MOFs by guest I_2.[18,19] The oxidative doping of the framework system is commonly due to the oxidation of metal ion of the frameworks.[18] However, the oxidative doping of MOFs is not straightforward if the oxidation of metal ion of the frameworks is not feasible thermodynamically. In such systems, oxidative doping of the frameworks could be due to guest I_2–ligand π electron interaction. Although host–guest chemistry of MOF–I_2

Received: June 2, 2015
Accepted: July 30, 2015
Published: July 30, 2015

DOI: 10.1021/acsami.5b04771
ACS Appl. Mater. Interfaces 2015, 7, 18501−18507

systems and an improved electrical conductivity of the frameworks due to host I_2 molecules have been reported,[19] a detailed mechanism behind the oxidative doping of the frameworks has not been studied yet. In addition, after the oxidative doping, advantage of application of such MOFs with improved conductivity has been hardly investigated. In the present work, a thin film of Co-based MOFs, cobalt(II) 2,6-naphthalendicarboxylic acid (i.e., $Co_3(NDC)_3DMF_4$, which is denoted here as $Co_3(NDC)_3$), is investigated as a model MOF. The MOF films are deposited onto a nonconducting amine-functionalized glass substrate using layer-by-layer (LbL) and doctor-blade (DB) techniques. After iodine doping, the framework films are investigated for their electronic and semiconductor properties. The current work demonstrates that doping of iodine into the frameworks significantly improves the electrical conductivity within the frameworks. The detailed mechanism behind the improved conductivity of the iodine doped frameworks has been studied experimentally, and the observed results have been confirmed using the computational chemistry (DFT calculation) of the system. Further, as a concept-of-demonstration for application, it has been demonstrated that a facile transfer of photogenerated electron from the LUMO level of iodine doped $Co_3(NDC)_3$ to the conduction band of ITO or TiO_2 takes place, and the observed interfacial charge transfer phenomenon can be employed to harvest solar radiations.

2. EXPERIMENTAL SECTION

MOF thin films were prepared using doctor-blade and layer-by-layer techques. Details on the deposition procedures, iodine doping, film characterizations, and DFT calculations are given in the Supporting Information.

3. RESULTS AND DISCUSSION

Scheme S1 shows the progress of $Co_3(NDC)_3$ thin film formation using LBL and DB coating techniques. SEM images of the $Co_3(NDC)_3$ film on a glass substrate using DB (A) and LbL (B) coating techniques are shown in Figure 1, which

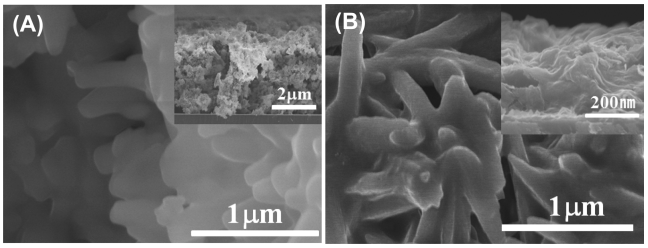

Figure 1. Top SEM view of $Co_3(NDC)_3$ MOFs: doctor-blade (A) and LbL (B) films. Insets show the cross-sectional SEM images of the respective films.

exhibit similar rod-like morphology of the frameworks in both films. However, the cross-sectional views of the films show that the LBL film has compact layers, while the DB film has microprous structure with large voids. The composition of the films determined by EDX is shown Figure S1. The XRD patterns of the bulk and the thin film of $Co_3(NDC)_3$ frameworks are shown in Figure 2. The diffraction patterns clearly show that the bulk $Co_3(NDC)_3$ synthesized by the standard solvothermal process[30] and the $Co_3(NDC)_3$ film grown by LbL and DB techniques have the same characteristic

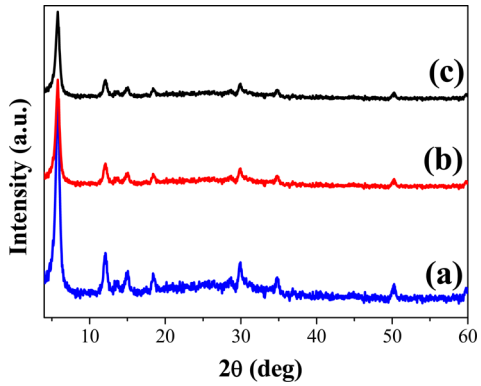

Figure 2. XRD patterns of $Co_3(NDC)_3$ MOFs: (a) bulk, (b) doctor-blade film, and (c) LbL film.

crystalline structure. This demonstrates the successful synthesis of thin MOF films.

$Co_3(NDC)_3$ films were further characterized using UV/visible absorption spectroscopy. $Co_3(NDC)_3$ framework layers on a glass slide show a characteristic absorption peak at about 548 nm in Figure 3A and Figure S2 (A), which is due to the d−d transition (i.e., t_{2g} (d7) to e_g transitions) associated with the Co^{II} centers of the frameworks. However, in addition to this peak, both of the films after iodine doping exhibited a new peak at about 438 nm. This peak position is exactly matching with the peak of iodine solution (Figure S2 (B)). Therefore, the peak at about 438 nm can be ascribed to the characteristic absorption peak due to iodine doping. Additionally, XPS was employed to investigate the doping of iodine into the frameworks. The XPS survey spectra of the as-prepared and doped films are shown in Figure S3 (A). The doped MOFs show I 3d XPS peaks (Figure S3 (A)), suggesting the capturing of iodine molecules inside the porous frameworks. Quantitatively, 0.35 molecules of iodine is found to be accommodated into 1 unit cell of $Co_3(NDC)_3$ frameworks. As reported previously,[19] capturing of iodine from iodine−acetonitrile solution was also noticed visually as well as by UV/visible absorption measurement (Figure S4). Figure 3B shows the electrical conductivity of the MOF films deposited on a glass substrate measured in terms of current passing through the film under an external voltage bias. Originally, the as-prepared MOF films without doping show the insulating behavior. However, regardless of the methods of film formation, the framework films after iodine doping allow the passage of currents under external bias. As compared to the DB film, the LBL film exhibited little higher conductivity, which could be due to the lower number of grain boundary present in the LBL film. It will be noteworthy here to discuss briefly that the electronic absorption peak and the absorption edge positions of the $Co_3(NDC)_3$ film before and after iodine doping are the same in Figure 3A. On the basis of these data, the $Co_3(NDC)_3$ film before and after doping should have a similar energy gap and electronic property. Therefore, the apparent insulating behavior of the undoped films could be due to extremely poor conductivity as a result of poor carrier concentration (supposed to be virtually zero carriers) in the undoped materials. Further, the electronic and semiconducting properties of the $Co_3(NDC)_3$ films were characterized using a Hall Effect measuring device. When the MOF films on a nonconducting glass were investigated, they exhibit a Hall Effect with the electronic conductivity in the range of 10^{-6} (LBL film) to 10^{-7}

DOI: 10.1021/acsami.5b04771
ACS Appl. Mater. Interfaces 2015, 7, 18501−18507

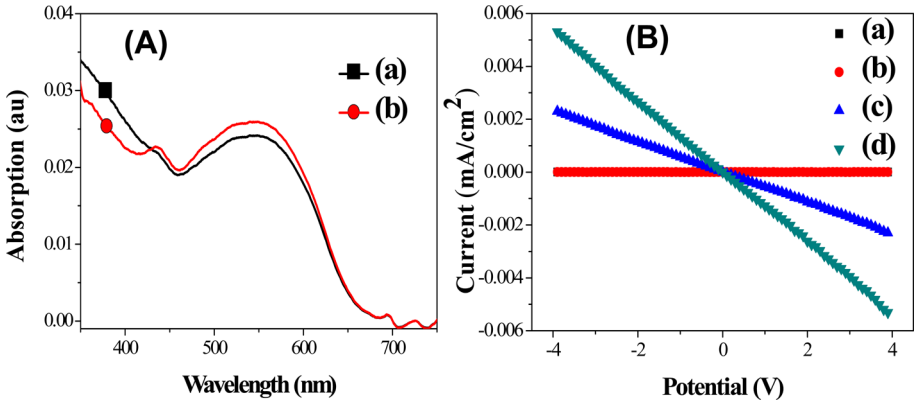

Figure 3. (A) UV/visible absorption spectra of $Co_3(NDC)_3$ MOF film on an amine-functionalized glass slide using LbL technique: (a) as-prepared and (b) iodine doped film. (B) Current vs applied bias curve of $Co_3(NDC)_3$ MOF films on a glass substrate: doctor-blade film without doping (a), LbL film without doping (b), doctor-blade film with iodine doping (c), and LbL film with iodine doping (d).

Table 1. Various Parameters Obtained at 25 °C from Hall Effect Measurement of $Co_3(NDC)_3$ MOF Films Prepared by Layer-by-Layer Technique on a Glass Substrate

bulk concentration	5.48×10^{11} (cm^3)	sheet concentration	1.64×10^7 (cm^2)
mobility	21.2 (cm^2/(V s))	conductivity	1.88×10^{-6} (s/cm^{-1})
resistivity	5.37×10^5 (Ω cm)	Hall coefficient	1.14×10^7 (m^2 C^{-1})

s cm^{-1} (DB film), the bulk charge carrier concentration in the range of ~+5 × 10^{11} cm^3, and the Hall coefficient in the range of ~+1 × 10^7 m^2 C^{-1} (Table 1, Table S1, and Figure S5 (A), (B)). As shown in Table 1 and Table S1, the conductivity of the LBL film is found to be a little higher than that of the DB film. In addition, when the undoped MOF films were investigated for the Hall Effect, the instrument displayed a "connection fail" message in the operating description window of the device monitor (Figure S5 (C)), which indicates that the electrical circuit for the measurement could not be established. This finding again suggests the insulating behavior of the undoped MOF films. These types of conductivity behaviors are in line with the current versus applied bias shown in Figure 3B. In addition to the electronic property, it should be noted in Table 1, Table S1, and Figure S5 (A),(B) that the bulk-charge carrier concentration and the Hall coefficient exhibited by the doped MOF films are positive, which implies that the doped MOFs are behaving as a p-type semiconductor. These results suggest that before iodine doping, the charge carrier concentration in the frameworks is virtually zero. However, iodine doping is working here as oxidative doping and, therefore, creating holes as charge carriers in the frameworks. The oxidation of the MOFs by iodine is also supported by the XPS detection of I_3^- (Figure S3(B)) in the iodine doped frameworks.

Each sub-building block unit of $Co_3(NDC)_3$ consists of a linear arrangement of three Co(II) ions linked via six carboxylate groups of the NDC ligands (Figure S6). The cross-linking of these trinuclear sub-building units via the naphthalene rings forms 1-D channels along the *a*- and *c*-axes, and thereby it produces a neutral 3-D network structure of the frameworks. The detailed structures of the $Co_3(NDC)_3$ can be found elsewhere.[30,31] The frameworks have shown dominating antiferromagnetic interactions between Co(II) ions of the frameworks perticularly in the high-temperature region, and a noticeable ferrimagnetic behavior in the low temperature region. The detail magnetic structure and property of the frameworks can be found in ref 31. During iodine doping, the iodine guest molecules are expected to be confined to the network structure of the frameworks surrounded by aromatic rings. Because of the intermolecular interactions between iodine guest molecules and π-electrons from the aromatic ring of the host, such arrangements can result in a cooperative charge transfer. Therefore, the observed conductivity of the iodine doped film can be considered as a result of interaction between iodine and the aromatic ring of the frameworks. The oxidization of Co^{2+} ion of the frameworks by iodine is thermodynamically not feasible due to their unfaborable redox potentials. This argument is also supported experimentally by XPS spectra of the frameworks before and after iodine doping in Figure S3(C), where no shift in binding energy positions of the Co 2p peaks before and after iodine doping can be observed. Instead of metal ions, probably the charge transfer interaction between iodine and ligand particularly with π-electrons from the aromatic ring of the ligands takes place, which leads to the oxidation of the frameworks, and thereby hole doping into the frameworks takes place. To confirm the above charge transfer reaction leading to oxidation of the aromatic ring, detailed studies on C 1s XPS spectrum of the frameworks were made. In contrast to the undoped frameworks, the deconvoluted C 1s peaks of the iodine doped frameworks show a small new peak at 285.5 eV, which is located at a higher binding energy position than the peak due to the C−C bond in Figure S3(D). This new peak can be ascribed to the consequence of charge transfer interaction between iodine and the aromatic ring of the ligands leading to the above readox reaction.[32] Further, Figure 4A shows the UV/visible absorption spectra of free I_2, and $Co_3(NDC)_3$ before and after iodine doping. A similar UV/visible spectrum can also be observed in the case of iodine doped naphthalene dycarboxylic acid (Figure 4B). In addition to the characteristic peak from iodine at about 512.8 nm, a new peak in the deep UV region (i.e., at about 241.5 nm) can be observed. This additional absorption peak of the doped materials can be assigned to the donor−acceptor charge transfer complex formation[33,34] (i.e., π electrons from aromatic ring donor and I_2 acceptor interaction). These findings clarify the above observed hole

DOI: 10.1021/acsami.5b04771
ACS Appl. Mater. Interfaces 2015, 7, 18501−18507

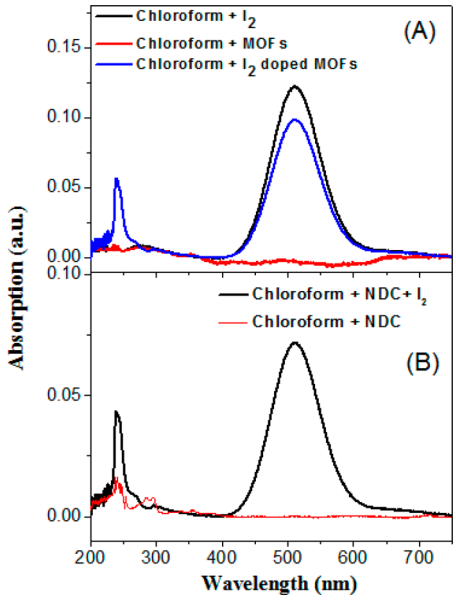

Figure 4. UV/visible absorption spectra of (A) iodine and saturated suspension of undoped and iodine doped $Co_3(NDC)_3$ MOFs in chloroform, and (B) iodine and saturated suspension napthalene dicarboxylic acid (NDC) in chloroform.

doping characteristic of the iodine doped $Co_3(NDC)_3$ films in Hall Effect measurements.

To further confirm the charge transfer-induced hole doping into frameworks by iodine doping, quantitative estimation of the charge transfer was performed using ab initio calculations based on DFT (for details, see Supporting Information SI-1). Results of the calculation are shown in Figure 5, which demonstrate that after iodine doping into $Co_3(NDC)_3$ MOFs, the HOMO level of the frameworks remains unchanged, and iodine levels appear over it (Figure 5A). In contrast, the LUMO level of the frameworks after iodine doping shifts down to

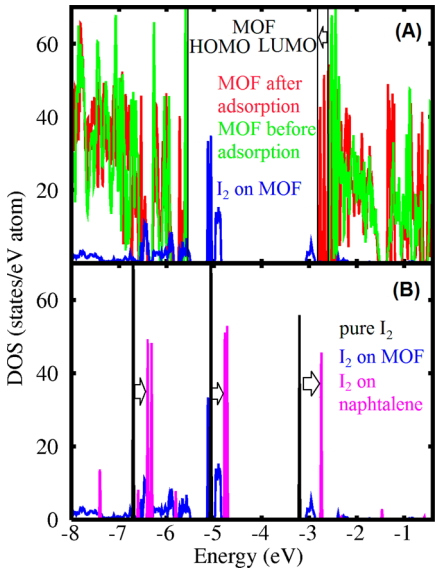

Figure 5. Total densities of states of $Co_3(NDC)_3$ MOFs with and without adsorbed iodine molecule (a), and iodine molecule adsorbed on $Co_3(NDC)_3$ MOFs, naphthalene dicarboxylic acid molecule, and free iodine molecule in empty box (b). Shifts of the positions of selected orbitals are indicated by arrows.

about 0.2 eV, which is attributed to the charge transfer from $Co_3(NDC)_3$ to I_2, and hole doping of the frameworks. Accepting electrons from $Co_3(NDC)_3$ or naphthalene dicarboxylic acid molecules also provides an almost similar energy level shift of the I_2 levels from the values of a pure I_2 molecule (Figure 5B). The observed shift is in qualitative agreement with the appearance of charge transfer complex formation in Figure 4 after iodine doping into $Co_3(NDC)_3$ and naphthalene dicarboxylic acid molecules. Note that a small quantitative difference in the shift of levels in the case of doping on naphthalene and $Co_3(NDC)_3$ can be observed, which is actually caused by the smearing of the energy levels of iodine on $Co_3(NDC)_3$ because, in contrast to naphthalene, the frameworks have bulk-like electronic structure. This is concluded on the basis of the almost identical value of transferred electrons and binding energies in both substrates. A similar calculated shift of the energy levels of iodine molecule has been reported to be in quantitative agreement with the shift calculated by quantum chemical methods after I_2 adsorption on benzene molecule.[35] The distance between iodine molecule and naphthalene rings (see Figure S6) is 3.28 Å for the case of adsorption on naphthalene dicarboxylic acid and 3.22 Å for adsorption on $Co_3(NDC)_3$ MOFs, which is smaller than typical van der Waals bonds (over 3.5 Å). The calculated value of binding energies for adsorption of I_2 on $Co_3(NDC)_3$ MOFs and naphthalene dicarboxylic acid is about 0.25 eV/I_2. This value is in order higher than typical values of van der Waals bonds (below 0.02 eV) due to enhancement of bond by charge transfer. On the other hand, the calculated value is smaller than the typical value of hydrogen bonds in water (0.43 eV/H_2O). So, we can conclude that at room temperature only part of the doped iodine molecules is adsorbed, forming a charge transfer complex with $Co_3(NDC)_3$ MOFs or naphthalene dicarboxylic acid. This conclusion is in good agreement with the results of measurements of the I 3d XPS spectrum (Figure S3(B)), which reveals that only one from about 6.7 iodine molecules adsorbed on MOFs with charge transfer. The total number of electrons transferred from MOFs or naphthalene to iodine molecule is about 0.02 electrons per I_2. Using the above data, we can estimate the number of holes induced in cm^3 of the MOFs by charge transfer complex with iodine as follows: (i) The volume of unit cell of $Co_3(NDC)_3$ MOFs is 5000 $Å^3$.[29] So, there are 2×10^{20} unit cells per cm^3. (ii) Experimental results demonstrate that there is about one I_2 per 3 unit cells (note that a unit cell contains 3 atoms of cobalt). Thus, there are about 6.6×10^{19} I_2/ cm^3. (iii) The concentration ratio of I_3^- (which participated in the formation of charge transfer bonds) and free I_2 is about 1:6.7, and thus the number of charge transfer per cm^3 of the frameworks is about 9.8×10^{18}. (iv) To calculate the total number of holes induced by charge transfer between MOFs and I_2, we multiply the obtained number by calculated value of transferred electrons (i.e., 0.02 electrons per I_2), and thus finally we obtain 1.9×10^{17} holes/cm^3 of the $Co_3(NDC)_3$ MOFs. The above calculated hole concentration is several orders higher than the experimental value obtained by Hall Effect measurement. The difference is due to the fact that we describe here a rather idealistic situation where all charge carriers are assumed to participate without any barriers from grain boundaries. However, in actual practice, the existence of lots of grain boundaries and other structural imperfections in MOF film resists electron transfer for the charge transfer complex formation. The current theory of mobility in 1D systems[36] demonstrates that its value depends on the elasticity of lattice

DOI: 10.1021/acsami.5b04771
ACS Appl. Mater. Interfaces 2015, 7, 18501−18507

and effective mass of charge carriers, which, on the other hand, depend on the shapes of the band structure. Adsorption of molecules does not affect elastic properties of MOF but can provide some changes in band structure. A more prospective source of the manipulation of mobility in doped MOF is the varying atomic structure of MOF that can provide dramatic changes in its band structure.

The semiconducting property of the MOF films is further characterized by measuring their HOMO−LUMO positions. Using the absorption spectra of the $Co_3(NDC)_3$ film, the optical band gap of iodine doped frameworks is estimated to be about 2.2 eV (Figure S7). The experimentally estimated energy gap of the doped frameworks is close to the calculated (about 2.1 eV) value. From the onset of ground-state oxidation peak in the cyclic voltammogram, the HOMO energy level is estimated to be −6.2 eV versus vacuum (Figure S8). On the basis of the energy gap and the HOMO energy level, the LUMO energy level of the $Co_3(NDC)_3$ frameworks is estimated to be about −3.9 eV. Recently, Butler et al.[37] have estimated HOMO−LUMO positions of a number of MOFs using DFT theory. However, the measured HOMO−LUMO energy levels of $Co_3(NDC)_3$ of the present work are different from those of other MOFs reported by them. As pointed out by them, some differences could arise from different methods used to measure the ionozation potentail. It shold be noted that the measured HOMO−LUMO energy levels of $Co_3(NDC)_3$ are closer to those of other transitional metal-based MOFs measured by the same cyclic voltammetric method.[38−40] Considering the strong visible light absorption characteristic of the frameworks as exhibited by Figure 3A and the suitable HOMO−LUMO positions, an interfacial electron transfer from LUMO level of the frameworks to a n-type material with lower conduction band such as ITO (−4.7 eV) or TiO_2 (−4.2 eV) could be established, and this phenomenon can be applied to light harvesting devices. To demonstrate this, a thin $Co_3(NDC)_3$ film was layered onto an ITO glass substrate, and TiO_2 film coated on a nonconducting glass substrate. The interfacial electron transfer phenomenon from the $Co_3(NDC)_3$ frameworks to the ITO or TiO_2 was studied using PL spectroscopy.

Figure 6 shows intense photoluminescence Co(II)* emission spectra of the undoped and doped $Co_3(NDC)_3$ films, which have exhibited a significantly higher photoluminescence quenching after iodine doping. The Co(II)* emission quenching can be attributed to an efficient interfacial electron transfer from LUMO of the frameworks to the conduction band of ITO. Quantitatively, the LBL and DB framework films have exhibited 97.4% and 95.1% of the Co(II)* emission quenching. A similar efficient interfacial electron transfer quenching phenomenon of the Co(II)* emission was also observed when the iodine doped $Co_3(NDC)_3$ frameworks are deposited to a TiO_2 film. The observed efficient interfacial electron transfer reveals the energy harvesting characteristic of the iodine doped frameworks. However, when a similar experiment was performed by layering a thin film of $Co_3(NDC)_3$ on a nonconducting glass substrate, no photoluminescence quenching was observed (Figure S9). This finding reveals the existence of a facile electron transportation path from cobalt d−d transition of the frameworks to the ITO or TiO_2 film only after iodine doping. The successful interfacial charge transfer after iodine doping of the frameworks can be ascribed to the improved conductivity of the frameworks by charge transfer-induced hole doping. The conductivity of the $Co_3(NDC)_3$ films after iodine doping is higher by a factor of 10^3 than that of the iodine.[18] As a result of the semiconducting behavior of the iodine doped $Co_3(NDC)_3$ film and its ability to inject photoelectrons into ITO or TiO_2, such materials could be used to construct a device that can be used in various fields. As an example of a demonstration, the observed interfacial charge transfer phenomenon is employed here to harvest solar radiations. For this, doctor-bladed TiO_2 mesoporous film on a FTO substrate was sensitized with $Co_3(NDC)_3$ layers using LBL techniques. After iodine doping, a Grätzel-type cell with a Pt counter and I^-/I_3^- redox electrolyte was constructed, and the light harvesting capability of the iodine doped $Co_3(NDC)_3$ layer was investigated in terms of the incident photon to current efficiency (IPCE). The IPCE spectrum shown in Figure S10 shows the maximum efficiency at the wavelength of the incident light where the absorption of light is maximum in the UV/visible absorption spectra (Figure 3A). This suggests that the $Co_3(NDC)_3$ film is working here as a light harvesting layer. As compared to the undoped film, the IPCE response in Figure S10 is attributed to the successful interfacial electron injection from the doped $Co_3(NDC)_3$ frameworks to the TiO_2 films.

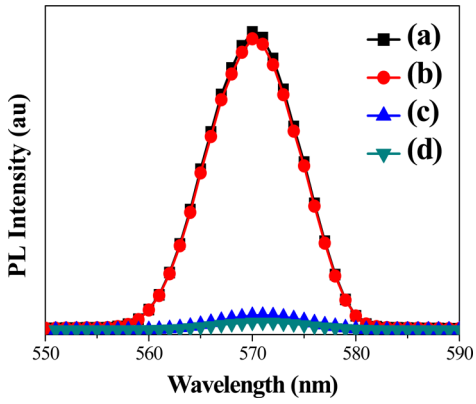

Figure 6. PL emission spectrum of (a) doctor-bladed undoped $Co_3(NDC)_3$ MOF film on ITO substrate, (b) undoped $Co_3(NDC)_3$ MOF LbL film on ITO, (c) doctor-bladed iodine doped $Co_3(NDC)_3$ MOF film on ITO, and (d) iodine doped $Co_3(NDC)_3$ MOF LbL film on ITO.

4. CONCLUSIONS

In summary, thin films of $Co_3(NDC)_3$ frameworks were fabricated using layer-by-layer and doctor-blade coating techniques, and the electrical conductivity of the films was improved significantly by iodine doping. In the current work, the undoped film shows insulating behavior, while the doped film exhibits a Hall Effect with p-type characteristic. The modification from insulator to p-type characteristic of the doped films is ascribed to the hole doping into the framework film due to the charge transfer complex formation. The HOMO−LUMO positions of the doped frameworks are found to be suitably situated for the efficient interfacial photoelectron injection from the frameworks to ITO or TiO_2. This result shows that the Co-based MOFs can be a potential new semiconducting material. As a large number of metal ions and a variety of organic linkers are available, an infinite number of combinations are possible to fabricate MOF films with further improved electronic and optical properties, which can have potential application in various fields.

DOI: 10.1021/acsami.5b04771
ACS Appl. Mater. Interfaces 2015, 7, 18501−18507

■ ASSOCIATED CONTENT

Supporting Information

The Supporting Information is available free of charge on the ACS Publications website at DOI: 10.1021/acsami.5b04771.

Experimental details on MOF film deposition, iodine doping, film characterization, DFT calculations, and additional results on characterization and application aspect of MOF films (PDF)

■ AUTHOR INFORMATION

Corresponding Authors

*E-mail: nabeenkshrestha@hotmail.com.
*E-mail: danil@hanyang.ac.kr.
*E-mail: shhan@hanyang.ac.kr.

Notes

The authors declare no competing financial interest.

■ ACKNOWLEDGMENTS

This research was supported by the KIST Institutional Program (2E23964) and by the Basic Science Research Program through the National Research Foundation of Korea (NRF) funded by the Ministry of Education (2013009768).

■ REFERENCES

(1) Czaja, A. U.; Trukhan, N.; Muller, U. Industrial Applications of Metal−Organic Frameworks. *Chem. Soc. Rev.* **2009**, *38*, 1284−1293.

(2) Choi, K. M.; Jeon, H. J.; Kang, J. K.; Yaghi, O. M. Heterogeneity within Order in Crystals of a Porous Metal−Organic Framework. *J. Am. Chem. Soc.* **2011**, *133*, 11920−11923.

(3) Deng, H.; Doonan, C.J.; Furukawa, H.; Ferreira, R. B.; Towne, J.; Knobler, C. B.; Wang, B.; Yaghi, O. M. Multiple Functional Groups of Varying Ratios in Metal-Organic Frameworks. *Science* **2010**, *327*, 846−850.

(4) Silva, C. G.; Corma, A.; Garcia, H. Metal−Organic Frameworks as Semiconductors. *J. Mater. Chem.* **2010**, *20*, 3141−3156.

(5) Gomes Silva, C. G.; Luz, I.; Llabres i Xamena, F. X.; Corma, A.; Garcia, H. Water Stable Zr−Benzenedicarboxylate Metal−Organic Frameworks as Photocatalysts for Hydrogen Generation. *Chem. - Eur. J.* **2010**, *16*, 11133−11138.

(6) Wang, D. E.; Deng, K. J.; Lv, K. L.; Wang, C. G.; Wen, L. L.; Li, D. F. Structures, Photoluminescence and Photocatalytic Properties of Three New Metal−Organic Frameworks based on Non-rigid Long Bridges. *CrystEngComm* **2009**, *11*, 1442−1450.

(7) Das, M. C.; Xu, H.; Wang, Z.; Srinivas, G.; Zhou, W.; Yue, Y. F.; Nesterov, V. N.; Qian, G.; Chen, B. A Zn_4O-Containing Doubly Interpenetrated Porous Metal−Organic Framework for Photocatalytic Decomposition of Methyl Orange. *Chem. Commun.* **2011**, *47*, 11715−11717.

(8) Lee, D. Y.; Yoon, S. J.; Shrestha, N. K.; Lee, S.-H.; Ahn, H.; Han, S.-H. *Microporous Mesoporous Mater.* **2012**, *153*, 163−165.

(9) Lee, D. Y.; Shinde, D. V.; Kim, E.-K.; Lee, W.; Oh, I.-W.; Shrestha, N. K.; Lee, J. K.; Han, S.-H. *Microporous Mesoporous Mater.* **2013**, *171*, 53−57.

(10) Hermes, S.; Schroder, F.; Chelmowski, R.; Woll, C.; Fischer, R. A. Selective Nucleation and Growth of Metal−Organic Open Framework Thin Films on Patterned $COOH/CF_3$-Terminated Self-Assembled Monolayers on Au (111). *J. Am. Chem. Soc.* **2005**, *127*, 13744−13745.

(11) Hermes, S.; Zacher, D.; Baunemann, A.; Woll, C.; Fischer, R. A. Selective Growth and MOCVD Loading of Small Single Crystals of MOF-5 at Alumina and Silica Surfaces Modified with Organic Self-Assembled Monolayers. *Chem. Mater.* **2007**, *19*, 2168−2173.

(12) Gascon, J.; Aguado, S.; Kapteijn, F. Manufacture of Dense Coatings of $Cu_3(BTC)_2$ (HKUST-1) on [alpha]-Alumina. *Microporous Mesoporous Mater.* **2008**, *113*, 132−138.

(13) Arnold, M.; Kortunov, P.; Jones, D. J.; Nedellec, Y.; Karger, J.; Caro, J. Oriented Crystallisation on Supports and Anisotropic Mass Transport of the Metal-Organic Framework Manganese Formate. *Eur. J. Inorg. Chem.* **2007**, *2007*, 60−64.

(14) Scherb, C.; Schodel, A.; Bein, T. Directing the Structure of Metal−Organic Frameworks by Oriented Surface Growth on an Organic Monolayer. *Angew. Chem.* **2008**, *120*, 5861−5863.

(15) Lu, G.; Farha, O. K.; Zhang, W.; Huo, F.; Hupp, J. T. Engineering ZIF-8 Thin Films for Hybrid MOF-Based Devices. *Adv. Mater.* **2012**, *24*, 3970−3974.

(16) Gandara, F.; Uribe-Romo, F. J.; Britt, D. K.; Furukawa, H.; Lei, L.; Cheng, R.; Duan, X.; O'Keeffe, M.; Yaghi, O. M. Porous, Conductive Metal-Triazolates and Their Structural Elucidation by the Charge-Flipping Method. *Chem. - Eur. J.* **2012**, *18*, 10595−10601.

(17) Talin, A. A.; Centrone, A.; Ford, A. C.; Foster, M. E.; Stavila, V.; Haney, P.; Kinney, R. A.; Szalai, V.; El Gabaly, F.; Yoon, H. P.; Léonard, F.; Allendorf, M. D. Tunable Electrical Conductivity in Metal-Organic Framework Thin-Film Devices. *Science* **2014**, *343*, 66−69.

(18) Kobayashi, Y.; Jacobs, B.; Allendorf, M. D.; Long, J. R. Conductivity, Doping, and Redox Chemistry of a Microporous Dithiolene-Based Metal−Organic Framework. *Chem. Mater.* **2010**, *22*, 4120−4122.

(19) Zeng, M. H.; Wang, Q. X.; Tan, Y. X.; Hu, S.; Zhao, H. X.; Long, L. S.; Kurmoo, M. Rigid Pillars and Double Walls in a Porous Metal-Organic Framework: Single-Crystal to Single-Crystal, Controlled Uptake and Release of Iodine and Electrical Conductivity. *J. Am. Chem. Soc.* **2010**, *132*, 2561−2563.

(20) Hendon, C. H.; Tiana, D.; Walsh, A. Conductive Metal−Organic Frameworks and Networks: Fact or Fantasy? *Phys. Chem. Chem. Phys.* **2012**, *14*, 13120−13132.

(21) Sun, L.; Miyakai, T.; Seki, S.; Dinca, M. Mn_2(2,5-disulfhydrylbenzene-1,4-dicarboxylate): A Microporous Metal−Organic Framework with Infinite $(-Mn-S-)_\infty$ Chains and High Intrinsic Charge Mobility. *J. Am. Chem. Soc.* **2013**, *135*, 8185−8188.

(22) Rao, K. V.; Datta, K. K. R.; Eswaramoorthy, M.; George, S. J. Light-Harvesting Hybrid Assemblies. *Chem. - Eur. J.* **2012**, *18*, 2184−2194.

(23) Kent, C. A.; Liu, D.; Ma, L.; Papanikolas, J. M.; Meyer, T. J.; Lin, W. Light Harvesting in Microscale MetalOrganic Frameworks by Energy Migration and Interfacial Electron Transfer Quenching. *J. Am. Chem. Soc.* **2011**, *133*, 12940−12943.

(24) Jin, S.; Son, H. J.; Farha, O. K.; Wiederrecht, G. P.; Hupp, J. T. Energy Transfer from Quantum Dots to Metal−Organic Frameworks for Enhanced Light Harvesting. *J. Am. Chem. Soc.* **2013**, *135*, 955−958.

(25) Zhan, W. W.; Kuang, Q.; Zhou, J. Z.; Kong, X. J.; Xie, Z. X.; Zheng, L. S. Semiconductor@Metal−Organic Framework Core−Shell Heterostructures: A Case of ZnO@ZIF-8 Nanorods with Selective Photoelectrochemical Response. *J. Am. Chem. Soc.* **2013**, *135*, 1926−1933.

(26) Gao, J.; Miao, J.; Li, P. Z.; Teng, W. Y.; Yang, L.; Zhao, Yanli.; Liu, B.; Zhang, Q. A p-Type Ti(IV)-based Metal−Organic Framework with Visible-Light Photo-Response. *Chem. Commun.* **2014**, *50*, 3786−3788.

(27) Campbell, M. G.; Sheberla, D.; Liu, S. F.; Swager, T. M.; Dinca, M. Cu_3(hexaiminotriphenylene)$_2$: An Electrically Conductive 2D Metal−Organic Framework for Chemiresistive Sensing. *Angew. Chem., Int. Ed.* **2015**, *54*, 4349−4352.

(28) Park, S. S.; Hontz, E. R.; Sun, L.; Hendon, C. H.; Walsh, A.; Van Voorhis, T.; Dinca, M. Cation-Dependent Intrinsic Electrical Conductivity in Isostructural Tetrathiafulvalene-Based Microporous Metal−Organic Frameworks. *J. Am. Chem. Soc.* **2015**, *137*, 1774−1777.

(29) Sun, L.; Hendon, C. H.; Minier, M. A.; Walsh, A.; Dincă, M. Million-Fold Electrical Conductivity Enhancement in Fe_2(DEBDC) versus Mn_2(DEBDC) (E = S, O). *J. Am. Chem. Soc.* **2015**, *137*, 6164−6167.

(30) Liu, B.; Zou, R. Q.; Zhong, R. Q.; Han, S.; Shioyama, H.; Yamada, T.; Maruta, G.; Takeda, S.; Xu, Q. Microporous Coordination Polymers of Cobalt(II) and Manganese(II) 2,6-Naphthalenedicarbox-

DOI: 10.1021/acsami.5b04771
ACS Appl. Mater. Interfaces 2015, 7, 18501−18507

ylate: Preparations, Structures and Gas Sorptive and Magnetic Properties. *Microporous Mesoporous Mater.* **2008**, *111*, 470−477.
(31) Wang, X.-F.; Zhang, Y.-B.; Zhang, W.-X.; Xue, W.; Zhou, H.-L.; Chen, X.-M. Buffering Additive Effect in The Formation of Metal−Carboxylate Frameworks with Slightly Different Linear $M_3(RCOO)_6$ Clusters. *CrystEngComm* **2011**, *13*, 4196−4201.
(32) Zhao, Y.; Wei, J.; Vajtai, R.; Ajayan, P. M.; Barrera, E. V. Iodine Doped Carbon Nanotube Cables Exceeding Specific Electrical Conductivity of Metals. *Sci. Rep.* **2011**, *1*, 83−87.
(33) Refat, M. S.; Grabchev, I.; Chovelon, J.-M.; Ivanova, G. Spectral Properties of New N,N-bis-alkyl-1,4,6,8-Naphthalenediimide Complexes. *Spectrochim. Acta, Part A* **2006**, *64*, 435−441.
(34) Camarota, B.; Goto, Y.; Inagaki, S.; Garrone, E.; Onida, B. Electron-Rich Sites at the Surface of Periodic Mesoporous Organosilicas: A UV−Visible Characterization of Adsorbed Iodine. *J. Phys. Chem. C* **2009**, *113*, 20396−20400.
(35) Su, J. T.; Zewail, A. H. Solvation Ultrafast Dynamics of Reactions. 14. Molecular Dynamics and ab Initio Studies of Charge-Transfer Reactions of Iodine in Benzene Clusters. *J. Phys. Chem. A* **1998**, *102*, 4082−4099.
(36) Beleznay, F. B.; Bogar, F.; Ladik, J. Charge Carrier Mobility in Quasi-one-Dimensional Systems: Application to a Guanine Stack. *J. Chem. Phys.* **2003**, *119*, 5690.
(37) Butler, K. T.; Hendon, C. H.; Walsh, A. Electronic Chemical Potentials of Porous Metal−Organic Frameworks. *J. Am. Chem. Soc.* **2014**, *136*, 2703−2706.
(38) Lee, D. Y.; Shinde, D. V.; Yoon, S. J.; Cho, K. N.; Lee, W.; Shrestha, N. K.; Han, S.-H. Cu-Based Metal−Organic Frameworks for Photovoltaic Application. *J. Phys. Chem. C* **2014**, *118*, 16328−16334.
(39) Lee, D. Y.; Shin, C. Y.; Yoon, S. J.; Lee, H. Y.; Lee, W.; Shrestha, N. K.; Lee, J. K.; Han, S.-H. Enhanced Photovoltaic Performance of Cu-based Metal-Organic Frameworks Sensitized Solar Cell by Addition of Carbon Nanotubes. *Sci. Rep.* **2014**, *4*, 3930−3934.
(40) Lee, D. Y.; Kim, E.-K.; Shin, C. Y.; Shinde, D. V.; Lee, W.; Shrestha, N. K.; Lee, J. K.; Han, S.-H. Layer-by-Layer Deposition and Photovoltaic Property of Ru-based Metal−Organic Frameworks. *RSC Adv.* **2014**, *4*, 12037−12042.

DOI: 10.1021/acsami.5b04771
ACS Appl. Mater. Interfaces 2015, 7, 18501−18507